Prediction Models of the final properties of steel rods obtained by thermomechanical rolling process

M. El Mehtedi, F. Pegorin, A. Lainati, S. El Mohtadi, S. Spigarelli

The objective of this research project was the setting up of a numerical model able to predict the microstructure of rod rolled products which, taking into account the rolling schedule and cooling, is able to provide the mechanical and microstructural final characteristics. The model was developed starting from the theoretical knowledge proposed by many researchers who have dealt with these issues, and the experience gained in the design of rolling systems by Siemens-VAI. In order to allow the maximum working flexibility to the final user, the prediction model requires to fill in the thermomechanical conditions for rod rolling (preheating temperature, reduction pass, rolling temperatures, interpass time, strain rate and cooling profile); a database of more than 150 steel types was developed, containing CCT curves and the mechanical properties relative to the cooling rates. The tool provides the CCT curves, suitably modified to take into account the microstructure of the rolled, superimposed with the cooling trajectory set up by the operator, as well as mechanical and microstructural data of interest for that particular class of steel. The Model was validated by direct comparison with the properties of rod rolled products under controlled conditions, obtaining an excellent prediction capability.

Keywords: Rod rolling - Prediction Models - CCT diagram - Mechanical properties - PAG

INTRODUCTION

The temperature, the deformation, the strain rate and cooling rate following the rolling can determine the technological characteristics such as to eliminate, in some products, subsequent costly thermal treatments. At the end of the rolling, the temperature of the workpiece is still very high, which depends both on the rolling system and the adopted rolling parameters. Modern technologies require constant monitoring of the temperature at different stages of the process, including the final cooling after the last rolling stand, and the evolution of the austenite grain size. The most interesting phases of the process are: a) rolling at a controlled temperature in the roughing mill and intermediate; b) upstream and downstream water cooling of finishing stands; c) controlled cooling of the evacuation lines.

For products in bars, cooling beds are used and properly proportioned in length and width, where the products, once discharged, are transported on special racks and processed during their movement by means of natural cooling, forced or delayed according to specification. For the products in coils, different evacuation lines are used, always equipped with cooling devices, such as air or water, and/or insulating hoods in case of necessity of slow cooling.

Mohamad El Mehtedi, Samer El Mohtadi, Stefano Spigarelli
DIISM, Università Politecnica delle Marche,
Via Brecce Bianche - 60123 – Ancona (Italy)
(corresponding author Mohamad El Mehtedi: elmehtedi@univpm.it)

Federico Pegorin, Alberto Lainati
Siemens – VAI MT, Marnate

A number of models describing various recrystallisation phenomena are available in literature. These models are sensitive to the applied strain, strain rate and deformation temperature besides austenitic grain size prior to deformation. Most of the researchers have used models available in literature and some have modified or developed their own [1-5]. Typically the models were validated by matching the mill loads or loads from laboratory trials. Since measuring the austenite grain size and its distribution in the rod during industrial hot rolling is impractical, the choice of microstructure evolution equations is dictated by the ability to predict the mill loads and final mechanical properties adequately. The CCT diagrams, containing the quantitative data pertaining to the dependence of steel structure and hardness on the temperature and time of the supercooled austenite transformations, are used for determination of the structure and the hardness of the steels after cooling at room temperature. Locations and shapes of the supercooled austenite transformation's curves, plotted on the CCT diagrams, depends mostly on the chemical composition of the steel, austenite grain size, as well as on austenitising temperature and time [6]; for this purposes, a database of more than 150 steel types was developed,

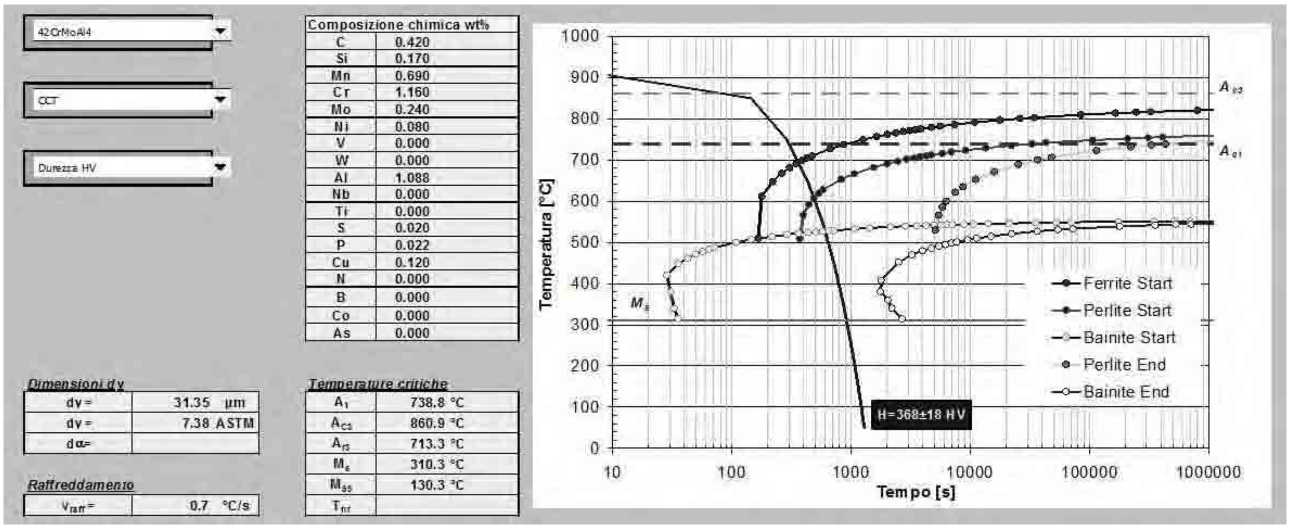

Fig. 1 - Selection screen of the material, with relative CCT diagram calculated according to the conditions set for the rolling schedule.

Fig. 1 - Schermata di selezione del materiale, con relativa curva CCT calcolata in base alle condizioni impostate per il ciclo.

containing CCT curves and the mechanical properties relative to the cooling rate.
The objective of the present research project, which is described herein the final product, was the setting up of a method of predicting the microstructure which, taking into account the conditions of rolling and cooling, would be able to anticipate the main mechanical and microstructural characteristics of the final product.

THE PREDICTION MODEL

The model was developed starting from the theoretical knowledge developed by many researchers who have dealt with these issues in the last decades [6-15]. In particular, the following aspects should be taken into account:

a. The effect of the chemical composition on the CCT curves and on the critical temperatures Ar3, Ar1 and Tnr
b. The effect of grain size on the position of the CCT curves
c. The extent of the deformation applied on each single rolling pass
d. The temperature and preheating time imposed on the material prior the rolling and the relative effect on the size of the starting austenitic grain
e. The interpass time
f. The possible presence of cooling system and the related laws of cooling imposed on the rolled material
g. The kinetics of static and dynamic recrystallisation between one pass and another (recrystallised fraction, kinetic constants, critical deformation for the onset of recrystallisation, temperature of non recrystallisation)
h. The kinetics of grain growth recrystallised statically or dynamically (see Appendix)

In order to allow a greater working flexibility to the user, the model requires to be fitted with the rolling working conditions (reduction for each pass, temperature, transfer time between stands, preheating temperature, possible cooling profile); the model includes a database of over 150 steel types, it contains the CCT curves and the mechanical properties in relation to the cooling rate. Once the steel is chosen from the database, the input data is set, the processing result is obtained in the form of a CCT diagram superimposed with the cooling trajectory set by the operator, as well as mechanical and microstructural data of interest for that particular class of steel (for example, ferrite grain size, hardness HV or HB, yield and ultimate stress for carbon steels). The calculation of the AGS after each rolling pass, which is a function of process parameters (imposed deformation in each stand and relative temperatures and strain rate, temperature and transfer time between stands, etc.., see Appendix) is obviously an important factor to estimate the position of the CCT curves, which move to the right as the austenite grain is coarser. Fig.1 shows an example of the output screen for the chosen steel (42CrMoAl 4). The screen shown in Fig.1 allows evaluating of some of the data calculated by the model, choosing as well the property of interest on the graph of the CCT diagram (this is given the Vickers hardness). A summary of the results of the calculation procedure is also provided in the form of a worksheet (Fig.2), which also shows, among other information, the input data relating to the rolling schedule.

EXPERIMENTS AND VALIDATION OF THE MODEL

For the experimental validation of the Model, Siemens-Vai carried out various rolling tests on site for 10 steels of different chemical compositions, in addition two different rolling schedules for steels S1 and S2 with different final finishing temperatures 960°C and 760°C were performed. The chemical composition in wt% of the studied steels is reported in Table 1. The samples were obtained from rolled bars (10 to 22 mm in diameter) according to the processing schemes; tensile tests and microhardness tests

Riepilogo

Step	T def. [°C]	v def. [s-1]	t iterg. [s]	ε
0				
1	1032	0.55	15.10	0.36
2	1014	0.62	12.30	0.34
3	1001	1.58	8.30	0.61
4	998	2.09	5.80	0.69
5	993	4.30	3.90	0.74
6	997	5.26	9.90	0.69
7	986	10.51	2.20	0.79
8	996	11.66	1.70	0.74
9	999	24.56	1.20	0.80
10	1013	27.99	1.50	0.76
11	1018	51.66	1.10	0.77
12	1033	57.09	1.50	0.74
13	1036	80.44	0.70	0.62
14	1043	83.83	2.70	0.61
15	1027	155.44	0.40	0.71
16	1042	160.36	0.30	0.69
17	1049	249.19	0.30	0.72
18	1063	263.30	5.60	0.70
19	956	345.75	0.01	0.50
20	965	397.80	0.01	0.54
21	972	402.96	0.01	0.32
22	971	397.14	1.80	0.29

Ciclo

Numero di passate	**22**

Preriscaldo

Temperatura [°C]	**1070**
Tempo [s]	**1793**

Raffreddamento

Tipo di raffreddamento	Costante	
Temperatura uscita raffreddatori [°C]	**950**	
Profilo di raffreddamento	T [°C]	t [s]
	950	1
	850	143.9
	750	286.7
	650	429.6
	550	572.4
	450	715.3
	350	858.1
	250	1001.0
	150	1143.9
	50	1286.7

Temperature critiche

A1	**738.8**	°C
AC3	**860.9**	°C
Ar3	**713.3**	°C
Ms	**310.3**	°C
M95	**130.3**	°C
Tnr		

Dimensioni del diametro austenitico

dγ =	**31.35**	μm
dγ =	**7.38**	ASTM
dα =		

Proprietà meccaniche

H	**350±17**	HB
H	**368±18**	HV
Rmax	**1154±58**	MPa
R0.2	**719±36**	MPa

Fig. 2 - Summary sheet in which it has been synthesised the input data related to the rolling schedule: deformation temperature (T_{def}), strain rate ($\dot{\varepsilon}$), interpass time (t_{ip}), strain (ε), temperature and time of preheating, cooling rate. The sheet also shows the final mechanical properties of the rolled.

Fig. 2 - Foglio di riepilogo in cui vengono sintetizzati i dati di input relativi al ciclo di laminazione: temperatura di lavorazione (T_{def}), velocità di deformazione ($\dot{\varepsilon}$), tempo intergabbia (t_{ip}), deformazione (ε), temperatura e durata di preriscaldo, curva di raffreddamento. Inoltre riporta anche le proprietà meccaniche finali.

steel	C	Mn	Si	P	S	Cu	Ni	Cr	Mo	W	V	Fe
S1	0.43	0.70	0.25	<0.01	<0.02	0.30	0.19	1.00	0.04	0.04	–	bal.
S2	0.49	0.73	0.23	<0.01	<0.02	0.25	0.13	0.08	0.04	0.02	–	bal.
S3	0.11	0.88	0.15	<0.01	<0.02	–	–	0.15	–	–	–	bal.
S4	0.09	0.46	0.16	<0.001	<0.02	–	–	0.04	0.03	0.02	–	bal.
S5	0.41	0.76	0.25	<0.001	<0.02	–	–	0.06	0.04	–	–	bal.
S6	0.29	0.84	0.04	<0.001	<0.01	–	–	0.44	0.04	0.04	0.13	bal.
S7	0.38	0.73	0.25	<0.001	<0.01	–	–	1.13	0.25	0.04	–	bal.
S8	0.85	0.87	0.23	<0.001	<0.01	–	–	0.24	0.03	–	–	bal.
S9	0.16	0.54	0.20	<0.001	<0.02	–	–	0.05	0.03	–	–	bal.
S10	0.57	0.79	1.73	<0.001	<0.01	–	–	0.13	0.02	–	–	bal.

Table 1 - Chemical composition of the studied steels (wt%).

Tabella 1 - Composizione chimica degli acciai studiati (peso%).

were carried out along the profile of the cross section; the microstructures were investigated by optical microscope, different etching solutions were used based on the carbon content of the steel.

It can be noted that for steel S1, the effect of finishing temperature is more significant than steel S2; in fact, contrary to what is expected, the hardness in steel S1 decreases by refining the austenite grain in the bars rolled at 760°C (see Figs. 3a and 3b); an explanation is, even if the refinement of austenite produced a finer ferrite-pearlite microstracture, the shift to the left of the cooling diagram CCT leads to a higher fraction of ferrite rather than pearlite at the same cooling rate. While the effect is negligible in the carbon steel S2 (Fig. 3c, 3d). The microstructure of the other steels is shown in figures 4.

In general, the predictive capabilities of the model appear to be more than adequate, as clearly shown in Fig.5 and Fig.6; for at least 8 of the 10 studied steels, the results of the predicted properties presented by the model are included in the ±10% band of the experimental values indicated by the dotted lines on the graphs. Taking into account the complexity of the production process and the micromea b c d

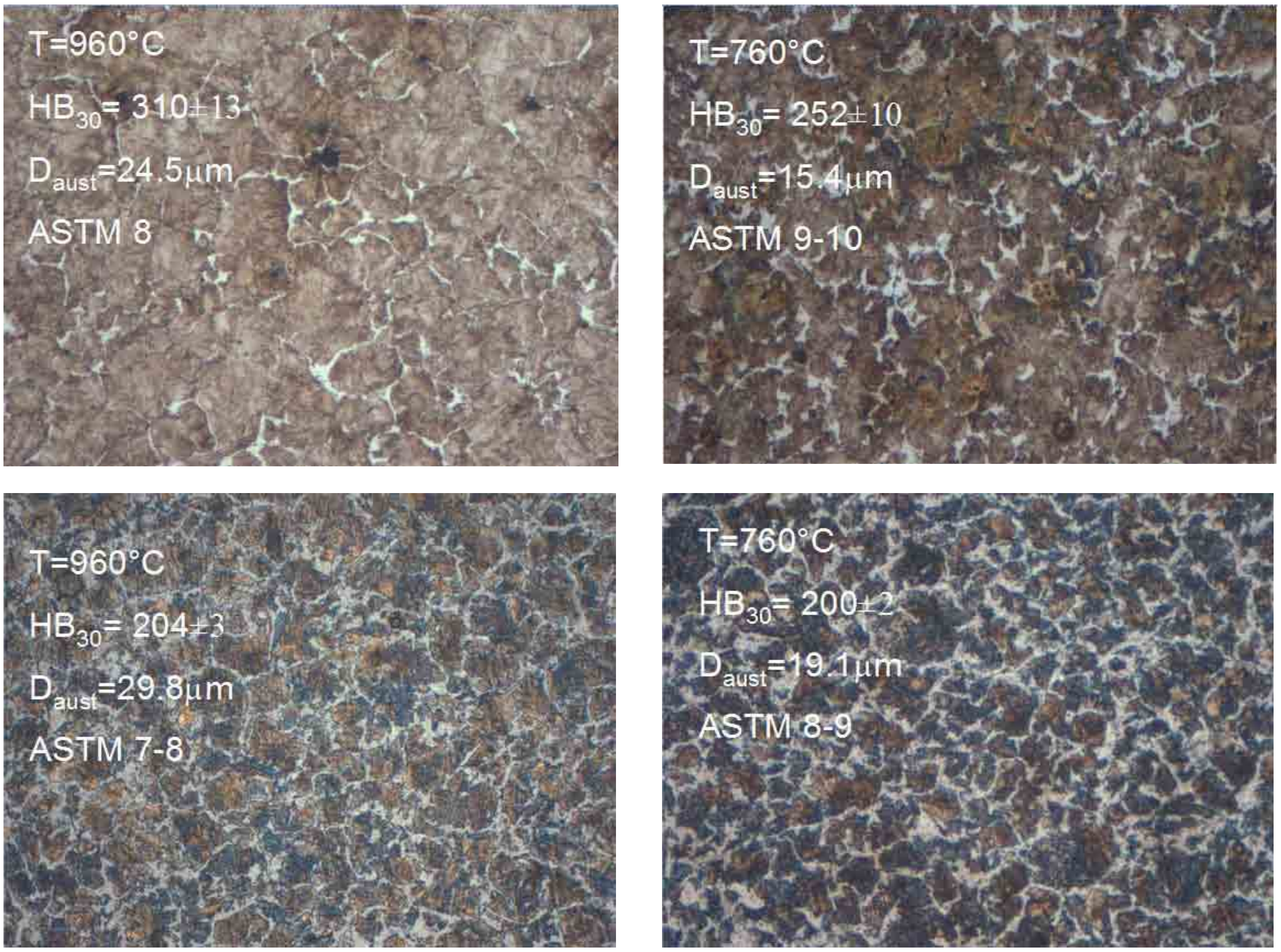

Fig. 3 - Microstructure of steel S1 (a,b) and S2 (c,d) rolled at 960°C and 760°C.

Fig. 3 - Microstruttura degli acciai S1 (a,b) e S2 (c,d) laminati a 960°C e 760°C.

chanisms involved during the rolling process, it is concluded that the model is able to provide a reliable prediction of the final mechanical properties after rolling process.

CONCLUSIONS

The prediction model developed during this research was particularly effective in estimating the effect of rolling parameters on the properties of rolled products. The model takes into account the complex kinetics of microstructural evolution taking place at various rolling stages, in order to provide an estimation of the austenitic grain size exiting the rolling mill. If the chemical composition plays an important role in determining the shape of the CCT cooling curves, the austenitic grain size causes a shift of these curves that can substantially affect the final microstructure. Considering all these factors and the cooling parameters imposed on the product, it is possible to estimate the mechanical properties that, in the most of the cases, differ by less than 10% from the experimental values. On this basis, it is possible to conclude that the model is sufficiently reliable to be used successfully in the design of rolling thermomechanical schedules of steels and allows optimising the rolling parameters in order to enhance or reduce some properties based on the customer needs.

APPENDIX: CONSTITUTIVE EQUATIONS USED FOR THE PREDICTION OF THE AGS DURING ROLLING

Once the thermo-mechanical parameters are calculated during the rolling process, the main problem is to calculate the average size of the austenitic grain and its evolution during the whole process.
The metadynamic recrystallisation (MRX) is the dominant microstructural phenomenon in many phases of the process. During the early rolling phases, the deformations per pass are usually very high, and it is easy for dynamic recrystallisation to occur. Further to the passes which impose deformations such as to cause a complete dynamic recrystallisation, the recrystallisation is not dynamic but metadynamic; this means that it starts while deformation is imposed and is completed in the transfer phase to the next rolling stand (interpass). In case of the finishing passes, the nominal deformations are below the critical value to start the DRX, while time is too short to promote the SRX. As a result, the deformations accumulate pass per pass, until they reach a critical value to initiate the dynamic recrystallisation. Over the years, several research

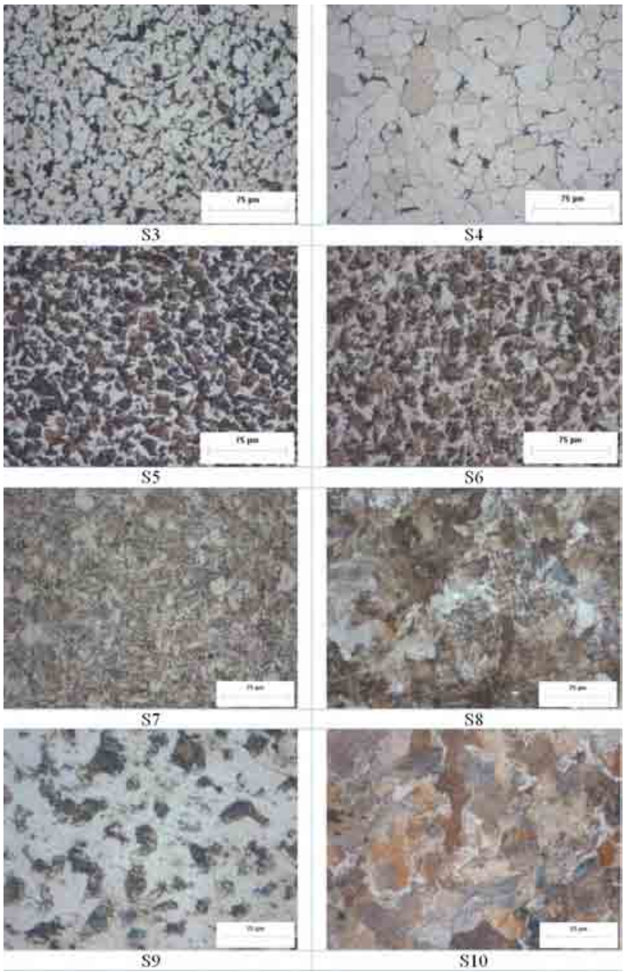

Fig. 4 - Microstructure of the steels obtained by OM.

Fig. 4 - Microstruttura degli acciai studiati vista al microscopio ottico.

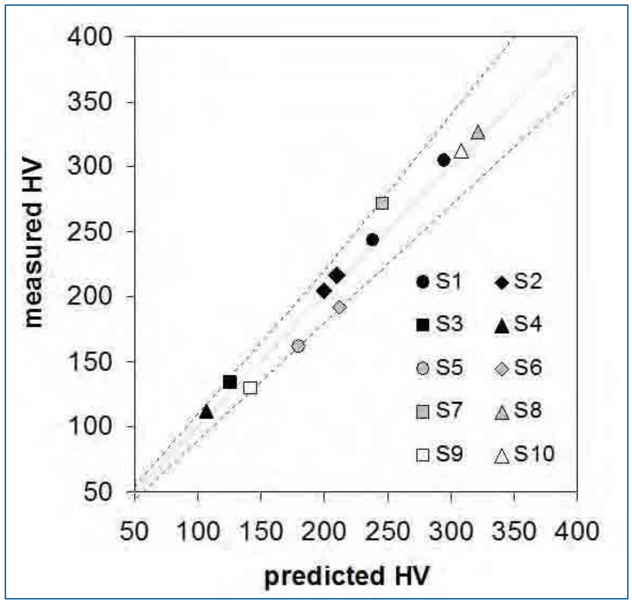

Fig. 5 - Comparison between the predicted hardness Vickers and the experimental one of the 10 steels.

Fig. 5 - Confronto fra le durezze calcolate dal modello e quelle sperimentali per i 10 acciai utilizzati per la validazione.

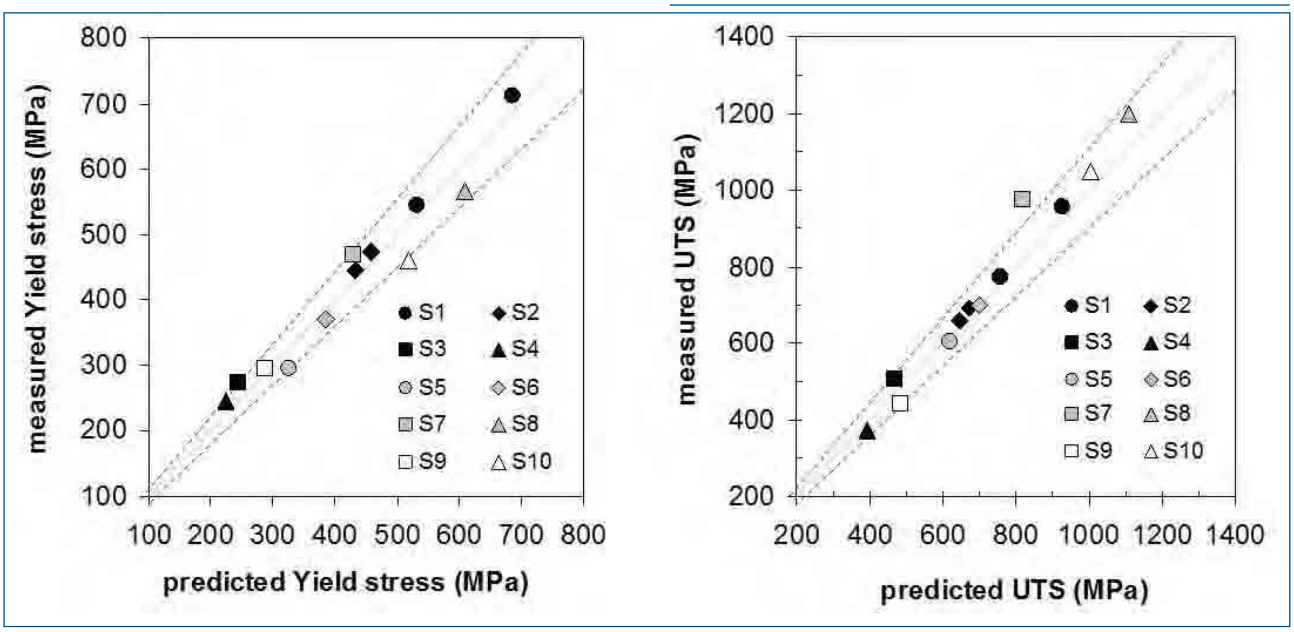

Fig. 6 - Comparison between the experimental ultimate strength (UTS) and the yield stress (0.2) and the calculated ones by the model.

Fig. 6 - Confronto fra la resistenza allo snervamento e la resistenza a trazione sperimentali e quelle calcolate dal modello per i 10 acciai utilizzati per la validazione.

Model	Equations
Critical strain	$\varepsilon_c = 5.6 \cdot 10^{-4} d_0^{0.3} Z^{0.17}$
Zener-Hollomon parameter (Z)	$Z = \dot{\varepsilon} \cdot exp(Q_{HW} / RT)$
Static recrystallisation	$X_R = 1 - exp\left[-0.693\left(\frac{t}{t_{0.5}}\right)\right]$ $t_{0.5} = 2.3 \cdot 10^{-15} \varepsilon^{-2.5} d_0^{2} exp\left(\frac{Q^I}{RT}\right)$
Metadynamic recrystallisation	$X_R = 1 - exp\left[-0.693\left(\frac{t}{t_{0.5}}\right)^{1.5}\right]$ $t_{0.5} = 1.1 Z^{-0.8} exp\left(\frac{Q^I}{RT}\right)$
Recrystallised grain size	
Static	$d_{SRX} = 343 \varepsilon^{-0.5} d_0^{0.4} exp\left(\frac{-Q^{II}}{RT}\right)$
Metadynamic	$d_{MDRX} = 2.6 \cdot 10^4 Z^{-0.23}$
Grain growth	if $t_{ip} > 1$ s
	$d^7 = d^7_{SRX} + 1.5 \cdot 10^{27} \left(t_{ip} - 4.32 t_{0.5}\right) exp\left(-Q^{III} / RT\right)$
	$d^7 = d^7_{MRX} + 8.2 \cdot 10^{25} \left(t_{ip} - 2.65 t_{0.5}\right) exp\left(-Q^{III} / RT\right)$
	if $t_{ip} < 1$ s
	$d^2 = d^2_{SRX} + 4.0 \cdot 10^{7} \left(t_{ip} - 4.32 t_{0.5}\right) exp\left(-Q^{IV} / RT\right)$
	$d^2 = d^2_{MRX} + 1.2 \cdot 10^{7} \left(t_{ip} - 2.65 t_{0.5}\right) exp\left(-Q^{IV} / RT\right)$
Partial recrystallisation	$d_{0,i+1} = X_{Ri}^{4/3} d_{RXi} + (1 - X_{Ri})^2 d_{0i}$ $\varepsilon_{a,i+1} = \varepsilon_{i+1} + (1 - X_{Ri}) \varepsilon_i$

groups have developed equations relate to the evolution of the austenitic grain size in hot rolling. A recent review is provided by Hodgson and Gibbs12. The equations utilised by the model in this study are presented above.

REFERENCES

1) M. Pietrzyk, C. Roucoules, P.D. Hodgson, Modelling the themomechanical and microstructural evolution during rolling of a Nb HSLA steel, ISIJ Int. Vol. 35-5, pp.531-541(1995).
2) D.Q. Jin, V.H. Hernandez-Avila, I.V. Samarasekera, J.K. Brimacombe, An integrated process model for the hot rolling of plain carbon steel, in: J. Beynon, P. Ingham, H. Teichert, K. Waterson (Eds.), Proceedings of the Second International Conference Modelling of Metal Rolling Processes, London, UK, December pp.36-58 (1996).
3) S.R. Wang, A.A. Tseng, Macro- and micro-modelling of hot rolling of steel coupled by a micro-constitutive relationship, Materials & Design 16(6), pp.315-336 (1995).
4) H. Dyja, P. Korczak, The thermal-mechanical and microstructural model for the FEM simulation of hot plate rolling, J. Mater. Process. Technol. 92-93, pp.463-467 (1999).
5) T. M. Maccagno, J. J. Jonas, P. D. Hodgson, Spreadsheet Modelling of Grain Size Evolution during Rod Rolling, ISIJ Int. Vol. 36, pp.720-728 (1996).
6) J.C. Zhao, M.R. Notis, Continuous cooling transformation kinetics versus isothermal transformation kinetics of steels: a phenomenological rationalization of experimental observations, Mater. Sci. Eng. R15, pp.135-207 (1995).
7) I. P. Kemp, Model of Deformation and Heat Transfer in Hot Rolling of Bar and Sections, J. Iron Making Steel Making Vol. 17, pp.139-143 (1990).
8) W. Lehnert, N. D. Cuong, Integrated Model for Calculating Microstructural and Forming Parameters of Steel during Rolling in Continuous Mills, ISIJ Int. Vol. 35, pp. 1100-1108 (1995).
9) Y. Lee, S. Choi, P.D. Hodgson, Analytical model of pass-by-pass strain in rod (or bar) rolling and its applications to prediction of austenite grain size, Materials Science and Engineering A Vol. 336 pp.177–189 (2002).
10) Y. Lee, S. Choi,Y. H. Kim, Mathematical Model and Experimental Validation of Surface Profile of a Workpiece in

Round-Oval-Round Pass Sequence, Journal of Materials Processing Technology. Vol. 108, pp.87-96 (2000).
11) Z. Wusatowski, Fundamentals of Rolling, Pergamon Press, London, pp.107-109 (1969).
12) P. D. Hodgson, R. K. Gibbs, A Mathematical Hot Rolled C-Mn Model to Predict and Microalloyed the Mechanical Properties of Steels, ISIJ Int. Vol. 32-12, pp.1329-1338 (1992).
13) C. M. Sellars, Modeling Microstructural Development during Hot Rolling, Mater. Sci. Technol. Vol. 6, pp.1072 (1990).
14) F. Boratto, et. al., Proc. Int. Conf. Physical Metallurgy of TMP of steels (THERMEC'08) Tokyo, pp.519 (1998).
15) M. El Mehtedi, F. Pegorin, S. Spigarelli, A. Lainati, Prediction tool of the qualitative characteristics of rolled products by controlling the thermomechanical parameters: Promet 4.0, Metallurgia Italiana, Vol. 104, Issue 9, pp. 5-11 (2012).

Modelli di previsione delle proprietà finali di tondini in acciaio laminati mediante processi termomeccanici

Parole chiave: acciaio - deformazioni plastiche - trattamenti termici - processi termomeccanici - modellazione - produzione - proprietà

La laminazione a caldo degli acciai non determina solo un cambiamento di forma del materiale lavorato, ma ne modifica sostanzialmente anche la microstruttura da cui dipendono le proprietà finali del prodotto. La temperatura, la velocità di deformazione e il raffreddamento successivo alla laminazione possono determinare caratteristiche tecnologiche tali da poter eliminare, in alcuni prodotti, successivi costosi trattamenti termici. Alla fine della laminazione il pezzo lavorato ha una temperatura ancora molto alta, che dipende sia dall'impianto che dai parametri di laminazione adottati. Le moderne tecnologie prevedono un controllo costante della temperatura nelle varie fasi del processo, incluso il raffreddamento finale dopo l'ultima gabbia in presa, e dell'evoluzione del grano austenitico. Le fasi più interessanti del processo sono: a. laminazione a temperatura controllata nel treno sbozzatore e intermedio; b. raffreddamento ad acqua a monte e a valle delle gabbie di finitura; c. raffreddamento controllato su linee di evacuazione. L'obiettivo di questo lavoro di ricerca è la messa a punto di un metodo di previsione della microstruttura che, tenendo conto delle condizioni di laminazione e raffreddamento, fosse in grado di anticipare le principali caratteristiche meccaniche e microstrutturali del prodotto finale. Il modello è stato sviluppato partendo dalle conoscenze teoriche sviluppate dai molti ricercatori che si sono occupati di queste problematiche. Al fine di consentire la maggiore flessibilità operativa all'utilizzatore, il modello prevede l'inserimento delle condizioni operative di laminazione. Il modello dispone di un database di oltre 150 acciai, contenente le curve CCT e le proprietà meccaniche in relazione alla velocità di raffreddamento.
Il modello è stato validato sperimentalmente mediante l'analisi delle proprietà meccaniche e microstrutturali di 10 acciai laminati su impianti industriali con diversi schemi di laminazione. Il modello di previsione si è rivelato particolarmente efficace nello stimare l'effetto dei parametri di laminazione sulle proprietà dei prodotti laminati. Il modello tiene conto delle complesse cinetiche di evoluzione microstrutturale che hanno luogo nelle varie fasi della laminazione, al fine di fornire una stima della dimensione del grano austenitico all'uscita del treno di finitura. Se la composizione chimica gioca un ruolo fondamentale nel determinare la forma delle curve di raffreddamento CCT, la dimensione del grano austenitico causa uno spostamento di tali curve che può avere sostanziali effetti sulla microstruttura e le relative proprietà meccaniche finali del laminato. Tenendo opportunamente in considerazione tutti questi fattori e dei parametri di raffreddamento imposti al laminato, si arriva ad ottenere stime delle proprietà meccaniche che, nella maggior parte dei casi studiati, differiscono meno del 10% dai valori sperimentali. Su queste basi, è possibile concludere che il modello è molto affidabile da poter essere utilizzato con successo nella progettazione di cicli di laminazione.